MAGNETIC RESONANCE – ELECTRICAL IMPEDANCE TOMOGRAPHY (MR-EIT): A new technique for high resolution conductivity imaging

B. Murat EYUBOGLU, Ozlem Birgul and Y. Ziya Ider
Dept. of Electrical & Electronics Engineering, Middle East Technical University, Ankara 06531 Turkey
E-mail: meyub@metu.edu.tr

Abstract*:* In this study, a new imaging modality for high resolution conductivity imaging is proposed. Both, the surface potentials and the magnetic fields produced by the probing current are measured. Surface potentials are measured by using conventional electrical impedance tomography techniques and high resolution magnetic field measurements are performed by using magnetic resonance imaging techniques. The conductivity distribution is reconstructed iteratively, to minimise the difference between the current densities calculated based on the potential measurements and the magnetic filed measurements. The proposed technique was tested on simulated data with/without simulated noise and it has been shown that absolute conductivity images with high resolution can be reconstructed.

1. INTRODUCTION

Electrical properties of biological tissues differ between tissues and for some tissues, these properties vary with physiological activity. This makes imaging of tissue conductivity values and physiological activity possible[1] and to serve this purpose, electrical impedance tomography (EIT) has been developed. In conventional EIT, surface measurements are used to reconstruct images of conductivity distribution inside a conductor object. Major drawbacks of EIT are low sensitivity of the surface measurements to conductivity perturbations in regions away from the measurement electrodes and poor quantitative accuracy [1]. Spatial resolution of EIT is also limited (worse than 10% of the array diameter) since the number of measurements are limited and the point spread function is not space invariant.

On the other hand, magnetic field and electrical current density in a volume conductor, created by current injection at the surface, can be imaged using magnetic resonance imaging (MRI) techniques, if the conductor contains magnetic resonance active nuclei [2-4]. This recently developed technique is called magnetic resosnance current density imaging (MRCDI) and with this technique dc [2-4] or radio frequency [5] currents and their magnetic field can be imaged with millimeter spatial resolution and high quantitative accuracy. A sensitivity based algorithm to reconstruct high resolution conductivity images using only the magnetic field measurements have been developed in [6]. However, absolute conductivity values can not be reconstructed with that method.

In this paper, a new imaging modality combining EIT and MRI techniques is presented. Sixteen electrodes are placed around the object to be imaged and the probing current is applied between opposite pairs of electrodes. Externally applied current produces an electric field which is a function of the electrical properties of the tissues in the body. Developed potentials are measured on the body surface at all electrodes other than the current injecting electrodes. In addition to the potential measurements, magnetic flux density inside the body is measured using MRCDI techniques. This process is repeated until all opposite pairs of electrodes are activated for current injection. An iterative algorithm is developed to reconstruct the conductivity distribution, minimising the difference between the current density distributions calculated based on the potential measurements and the magnetic flux density measurements. The proposed technique was tested on simulated data and it has been shown that absolute conductivity images with high resolution can be reconstructed.

2. MEASUREMENT OF MAGNETIC FLUX DENSITY USING MRCDI TECHNIQUES

Static electric current applied to a conductor generates a constant magnetic field with flux density $\vec{B}_j$. If the current carrying conductor contains MR active nuclei, the component of the magnetic flux density parallel to the main magnetic field accumulates a phase term in the spin echo signal

$$S = \int_x \int_y M(x,y)\, exp\left\{ j \left[g \left(G_x xt + G_y yt_y \right) + gB_j T_c \right] \right\} dxdy \qquad (1)$$

Where, M(x,y) is the transverse magnetisation, $G_x x$, $G_y y$ are the magnetic field gradients applied along x and y axis respectively, t and t_y are the duration of these gradients, γ is the gyromagnetic ratio, $\vec{B}_j$ is the component of the current-induced-magnetic-flux-density parallel to the main imaging field and T_c is the duration of the current pulse [4]. Any phase inhomogeneities need to be eliminated to make the phase image represent only the phase initiated by the current flow. In order to achieve this, the phase image acquired with a current pulse is normalized by the phase image acquired without a current pulse. Then the phase component caused by the current injection can be expressed as

$$\Phi_{jn} = \gamma B_j(x,y)T_c \qquad (2).$$

The magnetic flux density $\vec{B}_j$ can be calculated based on equation (2). Current density is related to the magnetic flux density by Biot-Savart law,

$$\vec{J} = \mu_o^{-1}(\nabla \times \vec{B}) \qquad (3).$$

In order to calculate the current density in one direction, the components of the flux density in two orthogonal directions in the plane perpendicular to the direction of the current density are needed. To determine components of the current density in three orthogonal directions, components of the magnetic flux density in all three directions are needed. This is achieved by repeating the MR imaging sequence three times and each time aligning one of the three orthogonal axis of the object with the main imaging field.

3. IMAGE RECONSTRUCTION ALGORITHM

The conductivity image is reconstructed on a Finite Element (FE) grid which will be described in the following section. Image reconstruction algorithm is a three step iterative algorithm:

1. Algorithm starts with an initial estimate of the conductivity distribution. In the first step, the forward problem is solved to calculate the node potentials of the FE grid by using the initial conductivity estimate, the measured surface potentials (Dirichlet boundary conditions) and known probing currents (Neumann boundary conditions). Knowing the potentials at all nodes and the conductivity estimate, the potential gradient and the current density distribution are estimated,
2. Magnetic flux density distributions are obtained from the MRCDI measurements as described in section 2. This calculation is made only for the first iteration.
3. In the third step, a new conductivity distribution is estimated to minimise the error between the current density estimates calculated based on the potential measurements and the magnetic filed measurements. The error function to be minimised is defined as

   $$R = \sum_M \int_S \left\| \vec{J}_{EIT} - \vec{J}_{MR} \right\| dS = \sum_M \sum_j \int_S \left\| -\sigma_j \nabla \phi_{EIT} - \vec{J}_{MR} \right\| dS \qquad (4)$$

   Where *M* is the number of independent current injection patterns, j is the number of elements in the finite element model. Subscripts EIT and MR stand for values calculated based on EIT and MRCDI measurements, respectively. Conductivity estimates for each element, which minimises the total error defined by equation (4), is found by setting $\partial R / \partial \sigma_j$ equal to zero. Therefore, the new estimate of the conductivity is obtained as

   $$\sigma_j = -\frac{1}{\mu_o} \frac{\sum_M \int_{S_j} \nabla \phi \cdot \nabla \times B \; dS}{\sum_M \int_{S_j} \nabla \phi \cdot \nabla \phi \; dS} \qquad (5)$$

The above three steps are repeated replacing the initial conductivity estimate with the calculated conductivity estimate of the previous iteration. Iterations can be stopped when the error between the estimated conductivity distributions of successive iterations falls below a preset level but here 50 iterations were performed to observe the convergence behavior of the algorithm. The error between the measured and the calculated surface potentials,

$$e = \sum_M \frac{\left\| \phi_m - \phi_c \right\|}{\left\| \phi_m \right\|} \qquad (6)$$

is also calculated at each iteration. In equation (6), ϕ_m and ϕ_c are the surface potentials measured and calculated for the estimated conductivity distribution, respectively.

The image reconstruction algorithm is tested on simulated data for concentric and eccentric inhomogeneities with several initial estimates.

4. RESULTS ON SIMULATED DATA

A FE model with 289 nodes and 512 triangular elements is used to simulate the surface potential and magnetic flux density data for various conductivity distributions. First, the forward problem is solved to calculate the node potentials and the surface potentials for a given conductivity distribution and Neumann boundary conditions. Then the potential gradient in each element and the current density is calculated. The calculated current density distribution is used to calculate the simulated magnetic flux density distribution based on Biot-Savart law:

$$d\vec{B} = \frac{\mu_o}{4\pi}\left(\frac{J\,d\vec{l}\times\vec{R}}{R^3}\right) \tag{7}$$

The simulated surface potentials and the magnetic flux density measurements are then used to reconsruct images of conductivity distribution as described in section 3. Reconstructed image for a concentric inhomogeneity is given in Figure 1(a). Position of the actual inhomogeity is shown by dashed lines. Conductivity values of the background region and the inhomogeneity are 2×10^{-3} ve 4×10^{-3} S/cm, respectively. The image given in Figure 1(a) has been reconstructed by using a homogeneous conductivity of 1×10^{-3} S/cm as an initial guess. Error as defined by equation (6) as a function of iteration is given in Figure 1(b) for different initial condutivity estimates. All converges to the same value after approximately 30 iterartions.

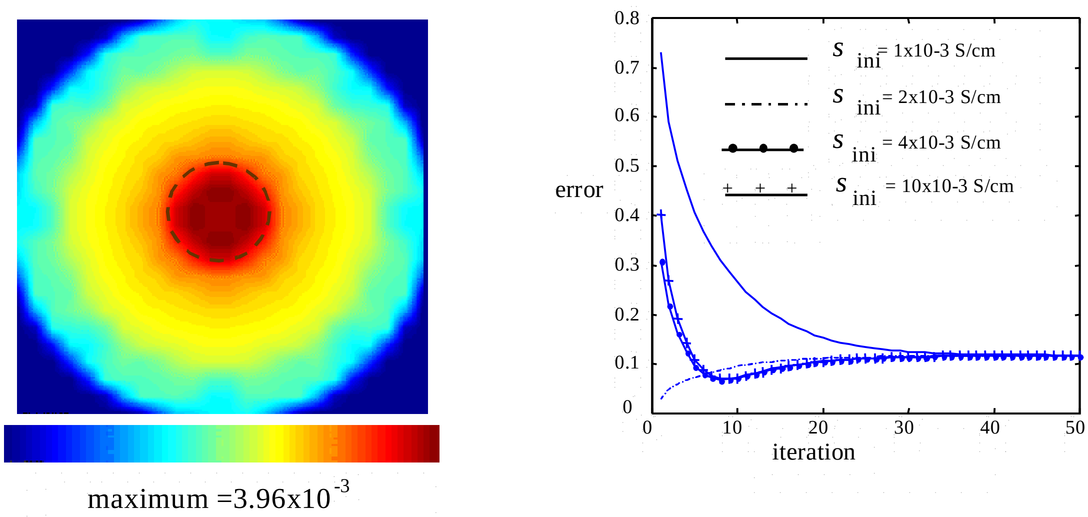

(a) (b)

Figure 1. (a) Reconstructed conductivity image for a concentric inhomogeneity, position of the actual inhomogenity is outlined by dashed lines, (b) error as a function of iteration, as described in equation (6).

Figure 2 (a) and (b) are the reconstructed image and the convergence plot for an eccentric conductivity distribution. Again the actual object location is shown by dashed lines. For both cases the position of the actual object is reconstructed correctly and the reconstructed values are close to the actual conductivity of the inhomogeneity after approximately 30 iterations. The quality of the reconstructed image is independent of the position of the inhomogeneity. However, in both cases the background conductivity is under estimated close to the electrodes. This results in an increased overall error. Reducing the FE grid size close to the electrodes may reduce this error.

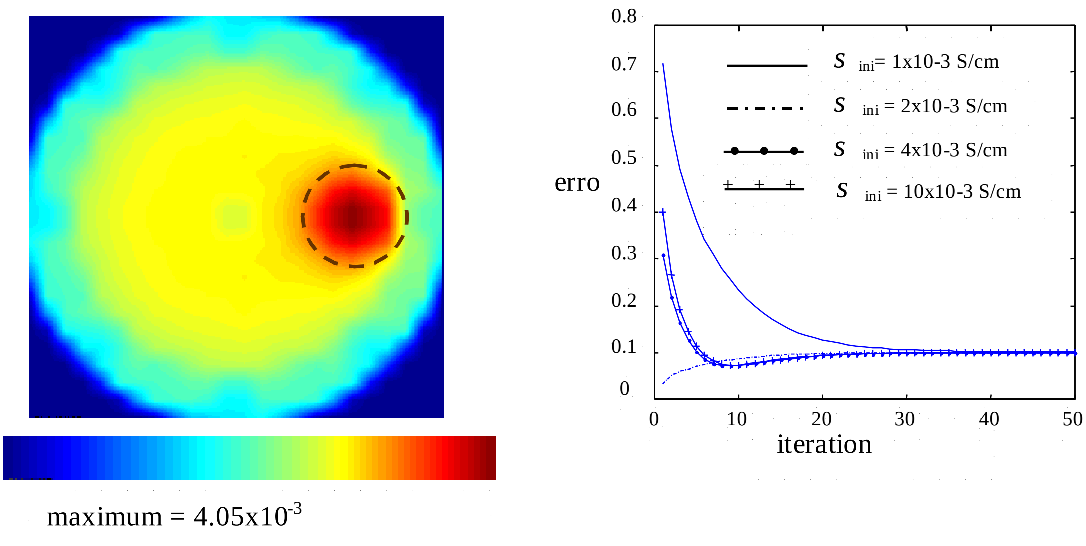

(a) (b)

Figure 2. (a) Reconstructed conductivity image for a eccentric inhomogeneity, position of the actual inhomogenity is outlined by dashed lines, (b) error as a function of iteration, as described in equation (6).

To investigate the noise performance of the proposed algorithm, simulated Gaussian noise with various standard deviations is added to the potentail data and the magnetic field data prior to the reconstruction. When noise with a maximum equal to 10% of the maximum potential measurement is added to the potential measurements and noise with a maximum equal to 10% of the maximum magnetic field measurement is added to the magnetic field measurements, the iteration error (as defined by equation (6)) is 24% for the eccentric inhomogeneity case, when the convergence is achieved. Better results obtained when the noise is added to only the potential or the magnetic field measurements and when the inhomogeneity is concentric.

5. CONCLUSIONS

In this study, combining the conventional EIT measurements and MRCDI measurements a novel imaging modality to reconstruct high resolution absolute conductivity images is proposed and tested on simulated data with/without noise. Further research is underway for practical implementation of the technique and optimization of the reconstruction algorithm. Future studies should involve the 3 dimensional implementation of the technique.

Acknowlegment: This work is supported by Turkish Scientific and Technical Research Council (TUBITAK) Research Grant EEEAG-198006.

References

1. K. Boone, D. C. Barber ve B. Brown, "Imaging with Electricity: Report of the European Concerted Action on Impedance Tomography", *Journal of Medical Engineering & Technology*, 21, no. 6, 201-232, 1997.

2. G. C. Scott, M. L. G. Joy, R. L. Armstrong ve R. M. Henkelman, "Measurement of Non-Uniform Current Density by Magnetic Resonance", *IEEE Trans. on Medical Imaging*, 10, no.3, 362-374, 1991.

3. G. C. Scott, M. L. G. Joy, R. L. Armstrong ve R. M. Henkelman, "Sensitivity of Magnetic Resonance Current Density Imaging", *J. Magnetic Resonance*, 97, 235-254, 1992.

4. B. M. Eyuboglu, R. Reddy ve J. S. Leigh, "Measurement of Electric Current Density with Magnetic Resonance Imaging", *IEEE Annual Medical Imaging Conference*, sayfa 1472-3, 1996.

5. G. C. Scott, M. L. G. Joy, R. L. Armstrong ve R. M. Henkelman, "Rotating Frame RF Current Density Imaging", *Magnetic Resonance in Medicine*, 33, 355-369, 1995.

6. Birgul O., Ider Y.Z., 1996, Electrical impedance topmography using magnetic field generated by internal currents, *IEEE Engineering in Medicine and Biology, 18th Conference, CD-ROM*.